Mononuclear Fe(II)-N4Py complexes in oxidative DNA cleavage

Li, Qian; Berg, Tieme A. van den; Roelfes, Gerard; Feringa, Bernard

Published in:
Dalton Transactions

DOI:
10.1039/b927145g

Publication date:
2010

Mononuclear Fe(II)-N4Py complexes in oxidative DNA cleavage: structure, activity and mechanism†

Qian Li, Tieme A. van den Berg, Ben L. Feringa* and Gerard Roelfes*

Received 24th December 2009, Accepted 8th June 2010
First published as an Advance Article on the web 26th July 2010
DOI: 10.1039/b927145g

A series of monotopic N4Py (*N*,*N*-bis(2-pyridylmethyl)-*N*-bis(2-pyridyl)methylamine, **1**) derived ligands have been prepared and evaluated in the iron catalyzed oxidative cleavage of pUC18 DNA, in the presence and absence of external reducing agent DTT. The mononuclear iron(II) complexes induce efficient DNA cleavage in air with a low catalyst loading. It was demonstrated that covalent attachment of 9-aminoacridine, ammonium group or 1,8-naphthalimide leads to increased DNA cleavage activity in the presence of a reductant. Also some complexes displayed a small degree of double-strand DNA cleavage activity. In contrast, in the absence of reducing agent, no beneficial effect of the covalently attached DNA binding moieties was observed, which was attributed to the reduction from Fe(III) to Fe(II), which is required for oxygen activation, becoming rate limiting. Mechanistic investigations revealed an important role for superoxide radicals. A proposed mechanism involves the formation of an Fe(III)–OOH intermediate as the active species or precursor.

Introduction

Bleomycins (BLMs) are a family of natural antibiotics produced by *Streptomyces verticillus* that are clinically used in the treatment of certain cancers, *e.g.* cancers of the cervix, head, neck and testicles.[1–5] Among this class of over 200 structurally related compounds, the administered form of BLMs, Blenoxane, mainly consists of bleomycins A_2 and B_2.[6] The clinical efficacy of BLMs is believed to derive from their ability to mediate DNA scission oxidatively, involving both single- and double-strand DNA cleavage, with the latter thought to be the major contributor to the cytotoxicity since single-strand DNA cuts are repaired by the cellular repair mechanisms much more efficiently than double-strand DNA cuts.[7–9] Double-strand DNA cleavage is the result of two successive strand scissions on opposite DNA strands in close proximity to each other.[10]

The mechanisms of bleomycin activation in the presence of metal ions and O_2 and the resulting DNA oxidation have been investigated extensively.[11] Fe–BLM was the first of the metallobleomycins demonstrated to effect DNA cleavage and showed the highest activity *in vitro*.[2] Inspired by the BLMs, a whole range of synthetic DNA-cleaving agents have been developed.[12–23] Many of these model complexes have proven to be capable of cleaving DNA in the presence of an iron salt and O_2, however, all of them only induced single-strand DNA cleavage.[24]

In our group, the pentadentate ligand *N*,*N*-bis(2-pyridylmethyl)-*N*-bis(2-pyridyl)methylamine (N4Py, **1**; Fig. 1) was designed and synthesized as a mimic of the metal-binding domain of BLMs.[25–27] Its corresponding iron(II) complex has been shown to be capable of inducing DNA strand breaks with molecular oxygen as terminal oxidant without the need for an external reducing agent. In the presence of an added reductant, DNA cleavage activity was significantly increased, however, only single-strand DNA cleavage was achieved.[26] Recently, we reported on a series of ditopic and tritopic N4Py-derived ligands. With their corresponding iron complexes, direct double-strand DNA cleavage was achieved oxidatively with iron for the first time, which was attributed to the increased possibility of a simultaneous delivery of two oxidizing equivalents to the DNA helix.[29,30]

Our previous studies indicated that the DNA cleavage activity of Fe(II)–N4Py was enhanced by introducing a DNA binding moiety such as 9-aminoacridine or an ammonium group, which was attributed to the increased interaction of Fe(II)–N4Py and DNA because of the binding moiety.[26] Here, we present the results of a study on the structure and activity of a series of monotopic N4Py ligands with covalently attached DNA-binding moieties, *i.e.* 9-aminoacridine, ammonium or naphthalimide moieties, connected to the N4Py ligand *via* spacers of different length.[30,31] Furthermore, the mechanism of oxidative DNA cleavage induced by Fe(II)–N4Py complexes has been investigated by addition of a series of mechanistic probes.

Results

Synthesis of the ligands

The ligands employed in the present study are shown in Fig. 1. Propyl and hexyl groups were selected as 3- and 6-carbon linkers, respectively. Ligands **1** and **2** were synthesized following the procedures previously described by our group.[25,26] Ligands **3a–c** were prepared through reactions of mono- and di-carboxylic ester substituted N4Py's with diamines (Scheme S1†). The naphthalimide moiety was introduced by reaction of corresponding N4Py amines **3a–c** with 1,8-naphthalic anhydride in methanol to form **4a–c** in moderate yields (Scheme S1).

Stratingh Institute for Chemistry, University of Groningen, Nijenborgh 4, 9747AG, Groningen, The Netherlands. E-mail: B.L.Feringa@rug.nl, J.G.Roelfes@rug.nl; Fax: +31 50 3634296

† Electronic supplementary information (ESI) available: Syntheses and NMR spectra of ligands **3a–c** and **4a–c**; DNA cleavage with iron salts, Fe(II)–BLM and all Fe(II)–N4Py complexes in the present study; calculation of the rate constants k_{obs} and k^*; mechanistic investigation of Fe(II)–**1**. See DOI: 10.1039/b927145g

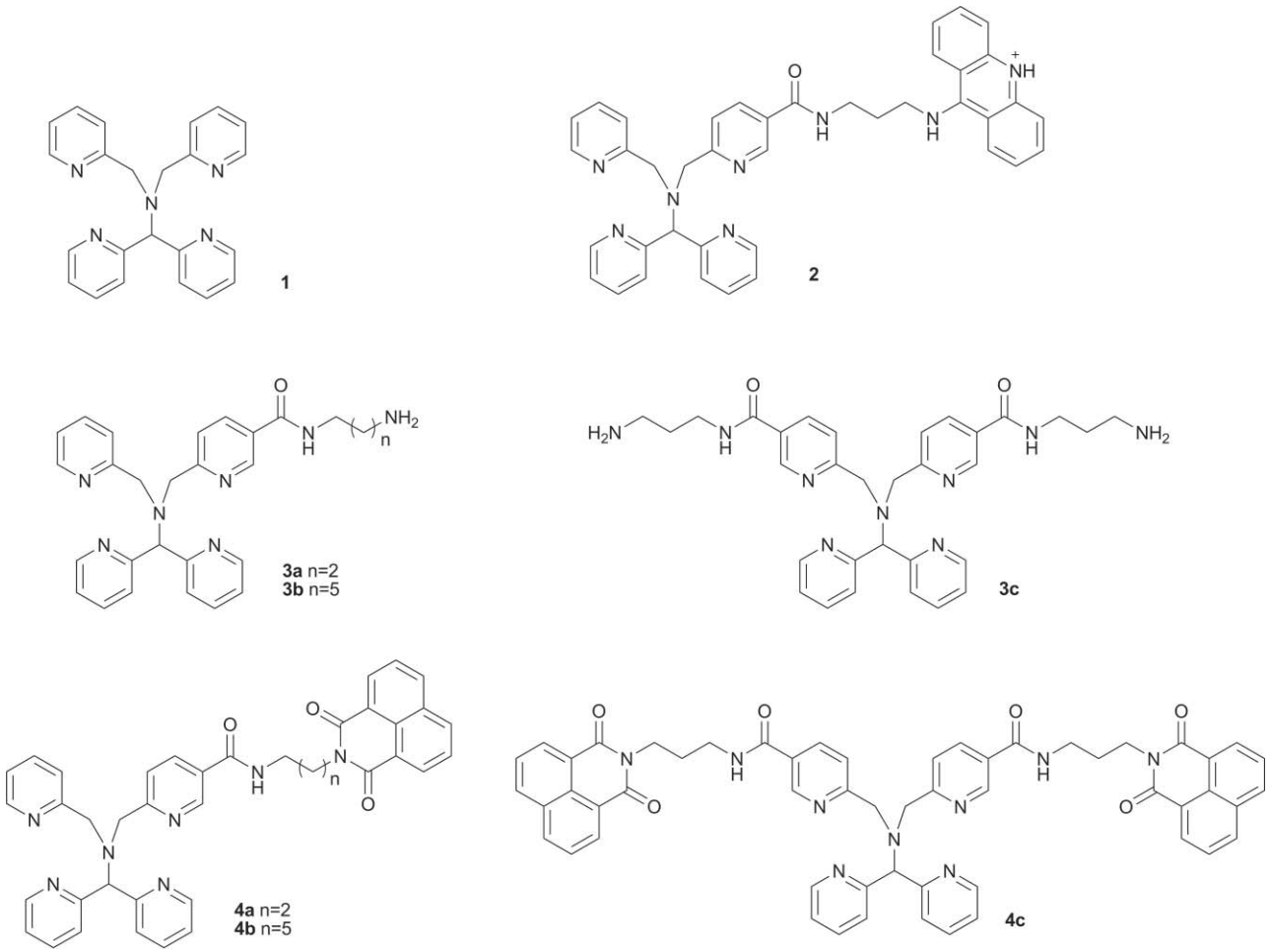

Fig. 1 Ligands employed in this study: N4Py and its mono-topic derivatives.

Complexation with iron

The iron(II) complexes of ligands **1** and **2** were prepared following procedures previously reported.[25,26] The corresponding iron(II) complexes of ligands **3a–c** and **4a–c** were generated *in situ* by complexation with $(NH_4)_2Fe^{II}(SO_4)_2{\cdot}6H_2O$ in water immediately prior to use for DNA cleavage. Previously, it has been established that one iron(II) is bound per N4Py unit, regardless of the substitution of the ligand.[25,26,28,29] Moreover, mono-nuclear iron(II) complexes of ligands **1**, **2** and **3a** have been isolated and characterized before.[25,26] For ligands **4a–c**, the formation of mono-nuclear iron(II) complexes was confirmed by ESI-MS (Table S1†).

DNA cleavage

It was reported that Fe(II) complexes of ligands **1** and **2** were capable of cleaving supercoiled Litmus29 plasmid DNA (0.1 μg μL^{-1}, 150 μM bp) at 1 μM concentration under air with no added reductants.[26] Here, to facilitate comparison of the activities of these mononuclear-complexes, also with multi-nuclear Fe(II) complexes reported before,[28,29] the DNA cleavage activities of the Fe(II) complexes of ligands **1–4**, were investigated by using supercoiled pUC18 (0.1 μg μL^{-1}) in 10 mM Tris·Cl buffer (pH 8.0) at 37 °C both in the presence and absence of 1000 equiv. dithiothreitol (DTT, 1 mM) with respect to iron. At this concentration the reaction is zero order in DTT (Figure S3†). The final concentration of the cleaving agents was 1 μM based on Fe(II), with a stoichiometry of 1 : 150 with respect to DNA base pairs, which corresponds to a catalyst loading of 0.7 mol %. All the experiments were carried out at least three times independently. For comparison, cleavage activities of iron salts and Fe(II)–BLM were investigated under the same reaction conditions.‡

DNA cleavage in the presence of reductant. DNA Cleavage activities of the Fe(II) complexes of ligands **1–4** were determined in the presence of DTT within 60 min (Table 1 and Figure S1†).

With all of these Fe(II)–N4Py complexes, efficient DNA cleavage, that is >30% conversion of supercoiled DNA within 5 min, was achieved. Except with Fe(II)–**1** and Fe(II)–**4b** (Table 1, entry 1 and 7), all supercoiled DNA was consumed completely within 40 min. The decrease of the supercoiled DNA fraction was accompanied by a steady increase in the fraction of nicked pUC18 DNA. Linear DNA was formed once a significant amount of

‡ In the absence of any iron source, a small amount of nicked DNA (<10%) was formed with DTT after 1 h, which resulted from the trace of metals in double distilled water. In the presence of DTT, BLM without added Fe^{2+} resulted in the formation of a comparable amount of nicked DNA (<10%), which should be attributed to both the trace of Cu–BLM in BLM and metals in aqueous solution. When DTT is absent in the reaction solution, no DNA cleavage was observed without any iron source.

Table 1 DNA cleavage in the presence and absence of DTT[a]

		With DTT					Without DTT			
No.	Complex	Time/min	Supercoiled DNA (%)	Nicked DNA (%)	Linear DNA (%)	ssc *vs.* dsc	Time/min	Supercoiled DNA (%)	Nicked DNA (%)	ssc *vs.* dsc
1	Fe^{II}–**1**	5	61 ± 4	39 ± 4	0	ssc	60	80 ± 1	20 ±1	ssc
		60	4 ± 1	88 ± 1	8 ± 2		120	79 ± 2	21 ± 2	
2	Fe^{II}–**2**	5	30 ± 2	70 ± 2	0	ssc	60	76 ± 1	24 ± 1	ssc
		60	0	—	—		120	64 ± 3	36 ± 3	
3	Fe^{II}–**3a**	5	47 ± 8	53 ± 8	0	ssc	60	77 ± 1	23 ± 1	ssc
		60	0	68 ± 3	32 ± 3		120	69 ± 1	31 ± 1	
4	Fe^{II}–**3b**	5	62 ± 5	37 ± 5	0	ssc	60	93 ± 1	7 ± 1	ssc
		60	0	82 ± 2	18 ± 2		120	90 ± 1	10 ± 1	
5	Fe^{II}–**3c**	5	55 ± 5	45 ± 5	0	ssc + dsc	60	77 ± 2	23 ± 2	ssc
		60	0	—	—		120	65 ± 2	35 ± 2	
6	Fe^{II}–**4a**	5	49 ± 5	51 ± 5	0	ssc	60	84 ± 1	16 ± 1	ssc
		60	0	83 ± 3	17 ± 3		120	83 ± 1	17 ± 1	
7	Fe^{II}–**4b**	5	73 ± 1	27 ± 1	0	ssc + dsc	60	93 ± 1	7 ± 1	ssc
		60	8 ± 2	84 ± 2	8 ± 2		120	92 ± 1	8 ± 1	
8	Fe^{II}–**4c**	5	60 ± 5	40 ± 5	0	ssc	60	97 ± 1	3 ± 1	ssc
		60	0	81 ± 3	19 ± 3		120	95 ± 1	5 ± 1	

[a] 1 μM iron complex, 0.1 μg μL^{-1} supercoiled pUC18 DNA (150 μM bp), 10 mM Tris·Cl buffer (pH 8.0), 37 °C, with or without 1 mM DTT. A correction factor of 1.31 is used to compensate for the reduced EtBr uptake capacity of supercoiled plasmid pUC18 DNA.[28]

nicked DNA (>60%) was present in the reaction. With Fe(II)–**1** and Fe(II)–**4b**, the fractions of linear DNA were 8% after 60 min, whereas with complexes Fe(II)–**3a**, Fe(II)–**3b**, Fe(II)–**4a** and Fe(II)–**4c**, considerably more linear DNA was obtained, *i.e.* between 17–32%. In the case of Fe(II)–**2** and Fe(II)–**3c**, more than 37% linear DNA was formed, which exceeded the limit for accurate quantification.[28,29]§

DNA cleavage pathway. Both single-strand and double-strand cleavage processes produce linear DNA. To distinguish these two cleavage pathways, the numbers of single-strand (*n*) and double-strand cuts (*m*) per DNA molecule were calculated for each reaction sample taken at different time points through statistical analysis using the formulas of Poisson distribution (Eqn (1) and (2)).[10,28,29] Fig. 2 shows the plots of the number of double-strand cleavage (*m*) *versus* the number of single-strand cleavage (*n*) for the Fe(II) complexes of ligands **1–4**. The dotted lines are the theoretical curves describing a pure single-strand cleavage pathway, which follow from the Freifelder–Trumbo relationship (Eqn (3)).[10]

For all the iron based reagents, values of *m* and *n* increased in time, which is consistent with the continued DNA cleavage within 60 min (Fig. 2). It is clear that complexes Fe(II)–**1**, Fe(II)–**2**, Fe(II)–**3a**, Fe(II)–**3b**, Fe(II)–**4a** and Fe(II)–**4c** are single-strand DNA cleaving agents since their *m*/*n* plots approximate the Freifelder–rumbo relationship, namely, the linear DNA that appeared in these DNA cleavage processes is the result of extensive single-strand cleavage. In the case of Fe(II)–**3c** and Fe(II)–**4b**, the *m*/*n* plots first approximate the Freifelder–rumbo relationship, but then deviate from it, indicating that initially only single-strand cleavage occurs, but that in a later stage double-strand cleavage also takes place. A similar pattern was observed with the di-nuclear Fe(II)–N4Py complexes reported previously.[28,29] This constitutes the first examples of mono-nuclear Fe(II) complexes capable of effective direct oxidative double-strand DNA cleavage, albeit that the double-strand cleavage activity is considerably lower than what was observed with multi-nuclear Fe(II)–N4Py complexes (Fig. 2d, Figure S2†) The cleavage pathways, single-strand cleavage (*ssc*) and single-strand cleavage (*ssc*) in combination with double-strand cleavage (*dsc*), for DNA cleavage by these complexes are listed in Table 1.

Rate of single-strand cleavage. For complexes which only induce single-strand cleavage, the average numbers of single-strand cuts per DNA molecule (*n*) can be calculated (Eqn (4) and (5)).[32] The calculated numbers were plotted against time and through the linear fit of the plot, the pseudo-first-order rate constants k_{obs} of single-strand cleavage process were obtained from the slope (Figure S6, Tables S2†).[32] In our study, the apparent pseudo-first-order rate constant k^* was used to describe the DNA cleavage efficiency of complexes (Table 2).[32] The value of k^* was obtained from k_{obs}, taking into account the concentrations of DNA and iron complex (Eqn (6)).

DNA cleavage processes effected by Fe(II)–**2**, Fe(II)–**3a** and Fe(II)–**4a** were faster than cleavage by Fe(II)–**1**, with a cleavage rate k^* of 2.1×10^{-2} min^{-1}, 1.2×10^{-2} min^{-1} and 8.2×10^{-3} min^{-1}, respectively, compared to 5.4×10^{-3} min^{-1} for Fe(II)–**1** (Table 2, entries 1–3, and 6). This clearly indicates the positive influence on DNA cleavage activity by the DNA binding moieties 9-aminoacridine, ammonium and naphthalimide. The DNA cleavage activity of Fe(II)–**3a** is intermediate between that of Fe(II)–**4a** and Fe(II)–**2**, suggesting that in addition to π–π stacking, electrostatic interactions play a key role in the binding and as a result the increase of DNA cleavage activity.

DNA cleavage in the absence of reductant. The DNA cleavage activities of the Fe(II) complexes of ligands **1–4** were investigated under the same reaction conditions within 2 h in the absence of reducing agent DTT as well. The results for the DNA cleavage with the Fe(II) complexes of ligands **1–4** are shown in Table 1 and Figure S7.†

§ The first term of the Poisson distribution predicts that the amount of linear DNA will reach a maximum at around 37%; in practice, this means smaller fragments of DNA are produced and as a result, a smear appears in the gel, which precludes quantitative analysis.

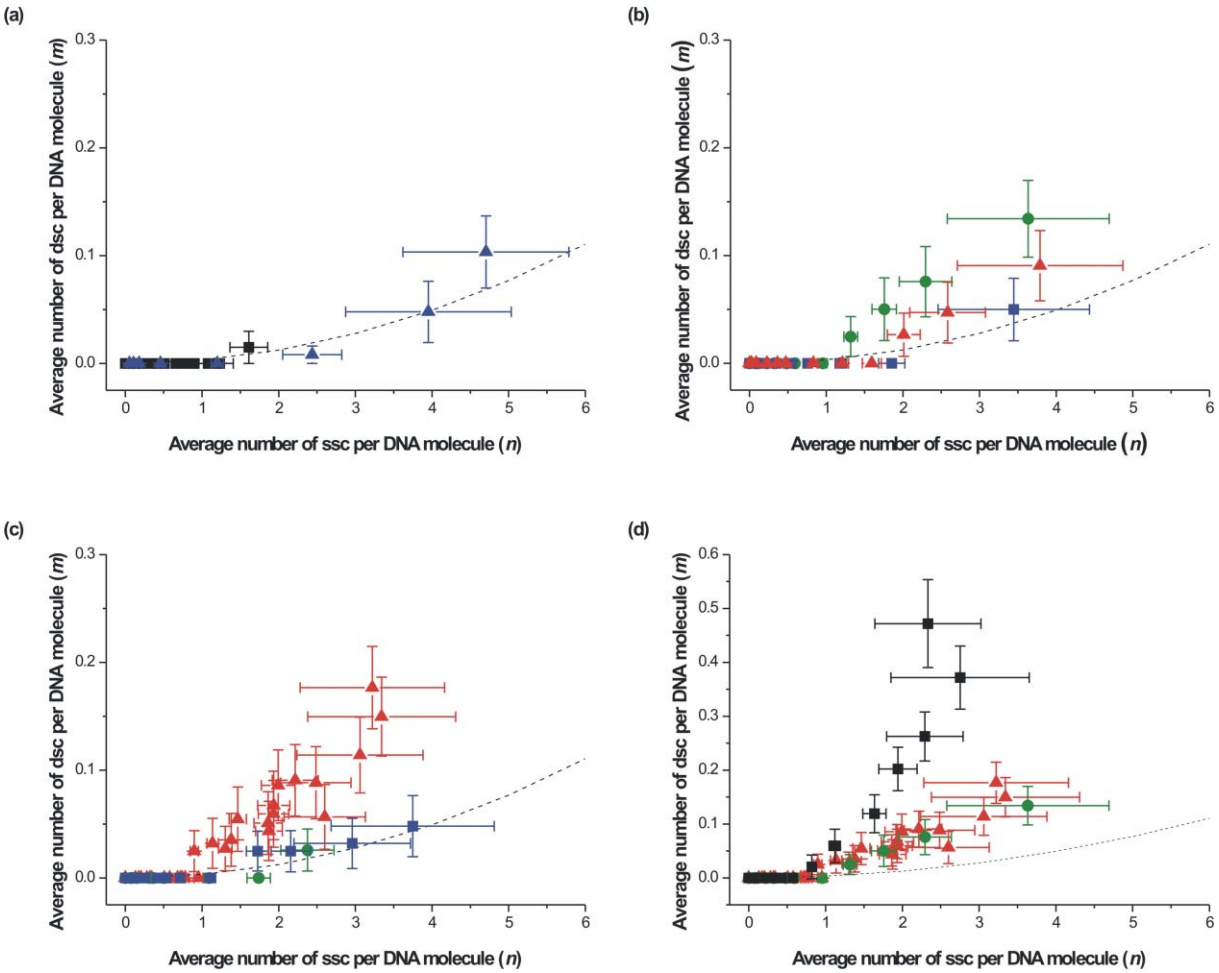

Fig. 2 Number of double-strand cuts (m) as a function of single-strand cuts (n) per DNA molecule for (a) Fe(II)–**1** (■) and Fe(II)–**2** (▲); (b) Fe(II)–**3a** (■), Fe(II)–**3b** (▲) and Fe(II)–**3c** (●); (c) Fe(II)–**4a** (■), Fe(II)–**4b** (▲) and Fe(II)–**4c** (●); (d) Fe(II)–**3c** (●), Fe(II)–**4b** (▲) and di-nuclear Fe(II)–N4Py complex Fe(II)–**L** (■)[32] Error bars represent the maximum and the minimum values of n and m. Dotted lines describe a pure single-strand cleavage pathway, as described by the Freifelder–Trumbo relationship.[10]

Table 2 The apparent pseudo-first-order rate constants (k^*) of DNA cleavage in the presence and absence of reductant

		$k^*/10^{-3}$ min^{-1}	
No.	Complex	With DTT	Without DTT
1	Fe^{II}–**1**	5.36 ± 0.17	0.197 ± 0.017[a]
2	Fe^{II}–**2**	21.4 ± 0.62	0.197 ± 0.006
3	Fe^{II}–**3a**	11.8 ± 0.51	0.164 ± 0.017
4	Fe^{II}–**3b**	8.01 ± 0.28	[b]
5	Fe^{II}–**3c**	6.88 ± 0.17[c]	0.186 ± 0.017
6	Fe^{II}–**4a**	8.18 ± 0.23[c]	0.158 ± 0.011[a]
7	Fe^{II}–**4b**	2.26 ± 0.06	[b]
8	Fe^{II}–**4c**	8.57 ± 0.28	[b]

[a] In the absence of DTT, with Fe(II)–**1**and Fe(II)–**4a**, the fraction of nicked DNA stopped increasing after 60 min so the rate constants are calculated for single-strand cleavage process within 60 min; [b] The cleavage rate cannot be obtained because of the small numbers of single-strand cuts. (Figure S8†); [c] In the presence of DTT, for double-strand cleaving agents Fe(II)–**3c** and Fe(II)–**4b**, only single-strand cuts (*ssc*) occurred before linear DNA was formed and rate constants for the single-strand cleavage process can be determined. With Fe(II)–**3c** and Fe(II)–**4b**, linear DNA appeared after 7.5 and 30 min, respectively.

In all the cleavage experiments with Fe(II) complexes of ligands **1–4**, only nicked and supercoiled DNA were present during the reaction, which means that all complexes exhibit single-strand DNA cleavage only. Moderate DNA cleavage, that is, formation of 17~36% of nicked DNA, was observed with Fe(II)–**1**, Fe(II)–**2**, Fe(II)–**3a**, Fe(II)–**3c** and Fe(II)–**4a**, whereas Fe(II)–**3b**, Fe(II)–**4b** and Fe(II)–**4c** produced significantly less nicked DNA (Table 1, entries 4, 7 and 8). The continuous increase in the amount of nicked DNA during 2 h with Fe(II)–**2**, Fe(II)–**3a** and Fe(II)–**3c** showed that these complexes remained active during this time. In contrast, with the rest of the Fe(II)–N4Py complexes, the formation of nicked DNA ceased increasing after 1 h, suggesting a deactivation of these complexes.

The numbers of single-strand cuts per DNA molecule (n) by Fe(II) complexes of ligands **1–4** at different time points were determined for each reaction sample by statistical analysis (Figure S8†).[32] From the linear fit of the data the pseudo-first-order rate constants (k_{obs}) of DNA cleavage were obtained (Table S2†) and then corrected to give k^* (Table 2).[32] The values of k^* for all complexes except Fe(II)–**3b**, Fe(II)–**4b** and Fe(II)–**4c**, were found

to be similar, from which it can be concluded that in the absence of reducing agent, the presence of DNA binding moieties has no favorable effect on the DNA cleavage activity. The extent of DNA cleavage observed with Fe(II)–**3b**, Fe(II)–**4b** and Fe(II)–**4c** was too small to allow accurate calculation of the cleavage rate under these conditions. This suggests that a longer spacer (6-carbon) and the second naphthalimide moiety affect DNA cleavage activity negatively.

DNA cleavage activity of Fe(II)–BLM. Under the same reaction conditions, Fe(II)–BLM is much more active and showed different DNA cleavage activity compared to its synthetic mimics. In the presence of DTT, a burst of DNA cleavage was observed within 20 s, which resulted in more than 80% of the supercoiled DNA being cleaved (Figure S9†). The DNA cleavage process was very slow after this initial burst of activity; the remaining 20% supercoiled DNA is cleaved during 30 min, which could indicate that decomposition of Fe–BLM under these conditions occurs. The *m*/*n* plot of the DNA cleavage with Fe(II)–BLM in the presence of DTT (Fig. 3) shows that the values of *m* jumped from 0 to 0.21 then stayed within a comparable region, while the values of *n* jumped from 0 to 1.5 and then slowly increased to 3.9. This suggests that double-strand DNA cleavage only occurs during the initial burst of DNA cleavage and that the slower cleavage process found after this initial burst is purely single-strand DNA cleavage. In the absence of DTT, a smear of the bands of different DNA forms on gel was observed, indicating substrate DNA was cleaved into small fragments, and as a consequence accurate quantification could not be obtained (Figure S10†). However, from the qualitative point of view, it can be concluded that the DNA cleavage with Fe(II)–BLM in the absence of DTT is less efficient than in the presence of DTT, and there is also a burst of cleavage at the beginning of the reaction. BLM is known to intercalate into DNA[33] and consequently it may be difficult for the complex to dissociate, which might account for the observed difference in DNA cleavage activity behaviour of Fe(II)–BLM after the initial burst.

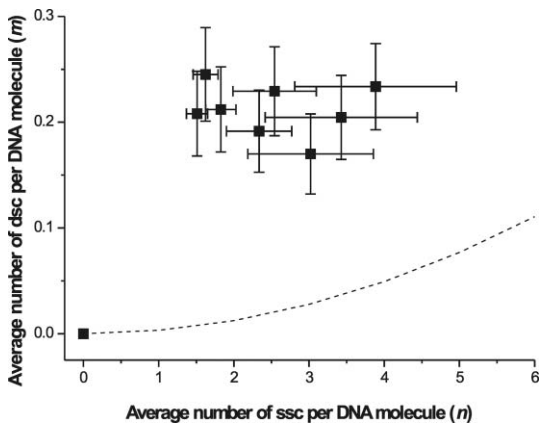

Fig. 3 Number of double-strand cuts (*m*) as a function of single-strand cuts (*n*) per DNA molecule for Fe(II)–BLM. Error bars represent the maximum and the minimum values of *n* and *m*. Dotted lines describe a pure single-strand cleavage pathway, as described by the Freifelder–Trumbo relationship.

Mechanistic probes

A series of mechanistic probes were added to the DNA cleavage reactions to gain insight into the nature of the reactive oxygen species (ROS) involved in the DNA cleavage effected by Fe(II)–N4Py complexes. The ROS scavengers that were used include superoxide dismutase (SOD), which converts superoxide radicals into O_2 and H_2O_2,[34] catalase, which converts H_2O_2 into O_2 and H_2O,[35] and dimethyl sulfoxide (DMSO), which acts as a hydroxyl radical scavenger.[36] These investigations were focussed on Fe(II)–**1**, which does not have a DNA binding moiety. In the case of complexes that are tightly bound to DNA, it may be difficult to intercept any reactive oxygen species with a scavenger before DNA damage occurs, which would potentially result in inaccurate mechanistic conclusions. The oxygen activation chemistry of the Fe(II) complexes of the N4Py based ligands **2**, **3a–c** and **4a–c** is unlikely to be different from that of the parent complex Fe(II)–**1**, which means that mechanistic conclusions for Fe(II)–**1** apply to the other Fe(II) complexes of N4Py-derived ligands as well.

Fig. 4 shows the average numbers of single-strand cuts (*n*) of Fe–**1** with different scavengers at 30 min in the presence and absence of DTT (Figure S14†). In the presence of DTT, the addition of catalase did not inhibit the activity of Fe–**1** (Figure S14a, lane 3), whereas the addition of SOD gave rise to a significant increase in cleavage activity (Figure S14a, lane 2). Addition of Bovine serum albumin (BSA) did not affect the activity (Figure S14a, lane 5), showing that the cleavage reaction is not sensitive to the presence of protein itself. These observations suggest an involvement of superoxide radicals in the cleavage process. The increase in activity

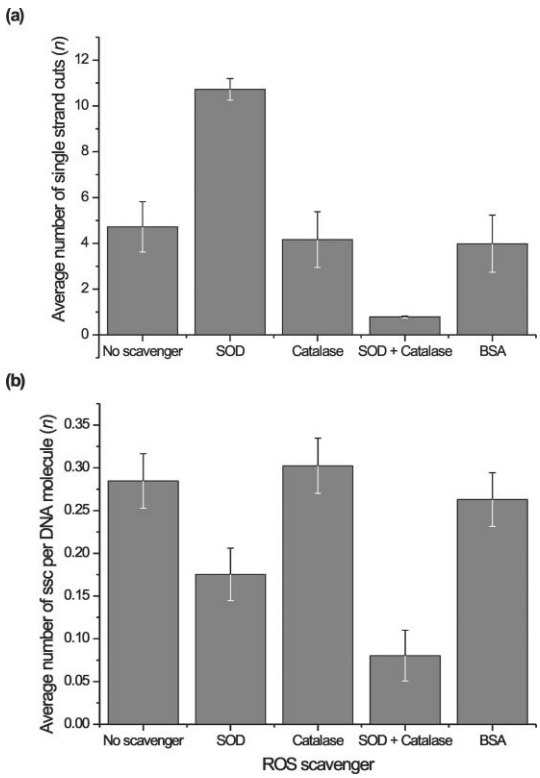

Fig. 4 Calculated average number of single-strand cuts per DNA molecule (*n*) with ROS scavengers at 30 min in the presence (a) and absence (b) of DTT.

of Fe–**1** with SOD is most likely due to the fact that the superoxide radicals formed in the reaction are converted into O_2 and H_2O_2. The latter is a much more potent oxidant (*vide infra*), resulting in more DNA cleavage. This is supported by the significant inhibition (~90%) that was observed when SOD and catalase were added together (Figure S14a, lane 4). In the absence of DTT, the addition of catalase and BSA did not inhibit the activity of Fe–**1** (Figure S14b, lane 3 and 5) and the addition of SOD resulted in a small drop (~40%) in the activity of Fe–**1** (Figure S14b, lane 2).[37] These observations also suggest an involvement of superoxide radicals in the cleavage process and a minimal effect of the presence of protein. A higher degree of inhibition (~70%) was also observed with SOD and catalase together (Figure S14b, lane 4) and the origin is probably the same as in the case of cleavage with DTT. No obvious effect on the cleavage activity was observed when 1000 equiv. DMSO with respect to Fe(II)–**1** was added (Figure S15, lane 3, 5, 7 and 9). This strongly suggests that hydroxyl radicals do not play an important role in the Fe(II)–**1** catalyzed DNA cleavage reaction, both in the absence and presence of DTT.

A dramatic increase in DNA cleavage was observed when 1000 equiv. of H_2O_2 with respect to Fe(II)–**1** were added (Figure S15,† lane 6). In the presence of DTT, accurate quantification of DNA cleavage was not possible due to the extensive DNA cleavage within 30 min (Figure S15, lane 8). In the absence of DTT, the amount of DNA cleavage obtained with Fe(II)–**1** and H_2O_2 was comparable to the case of Fe(II)–**1** and DTT (Figure S16†). The significant effect of H_2O_2 can be attributed to the formation of $[N4Py–Fe^{III}–OOH]^{2+}$ species.[25,38] This species, which has spectroscopic properties similar to "activated BLM", the low-spin BLM–Fe^{III}–OOH species that is believed to initiate the DNA cleavage reaction,[40–42] has been demonstrated before to be a very potent oxidant.[39]

Discussion

Effect of ligand structure on DNA cleavage activity

Fe(II)–N4Py complexes were demonstrated to be very efficient synthetic catalysts for oxidative DNA cleavage using O_2. In the presence of reducing agent DTT, the structure of the Fe(II)–N4Py complex affects its DNA cleavage activity significantly. With appended DNA binding moieties, the Fe(II)–N4Py complexes Fe(II)–**2**, Fe(II)–**3a**, Fe(II)–**4a** were found to have significantly higher DNA cleavage rates than Fe(II)–**1** (Table 2). Moreover, the nature of the DNA-binding moiety proved to be of importance. Fe(II)–**2**, which contains a 9-aminoacridine moiety, was proved to be the most efficient DNA cleaving agent. From comparison with Fe(II)–**3a** and Fe(II)–**1** it can be concluded that both hydrophobic and electrostatic effects contribute to the DNA-binding and, hence, DNA cleavage activity of Fe(II)–**2**. When incorporating two covalently linked ammonium or naphthalimide groups in the ligand, increased cleavage activity was observed. The spacer length also proved to be an important variable; the use of a 6-carbon instead of a 3-carbon linker gave rise to a decrease in cleavage efficiency. Special cases are Fe(II)–**3c** and Fe(II)–**4b**, which show a small but significant degree of double-strand cleavage activity. This represents the first examples of direct oxidative double-strand DNA cleavage by a synthetic mono-nuclear iron complex and, as such, is an attractive starting point for the development of the next generation of Fe–BLM mimics.

In the absence of DTT, DNA cleavage with Fe(II)–N4Py was much less efficient; cleavage rates k^* under these conditions were generally an order of magnitude lower (Table 2). Furthermore, no significant effect of ligand structure on activity was observed. A plausible explanation for this is that in the absence of external reducing agent, the reduction of Fe(III) back to Fe(II), which is required for oxygen activation, becomes rate limiting instead of the DNA oxidation. Indeed, the fact that the redox potential for the Fe(II)/Fe(III) couple of Fe(II)–**1** resembles those of Fe complexes of N4Py ligands containing a similar substitution at the pyridine rings[27] as ligands **2–4** explains why all complexes investigated here exhibit similar overall cleavage rates under conditions where reduction is rate limiting.

Nature of the active species

The experiments with scavengers for the reactive oxygen species demonstrated that superoxide plays a key role in the reaction mechanism of DNA cleavage catalyzed by Fe(II)-**1**. In the presence of an external reductant such as DTT, the presence of SOD significantly increased the reaction rate by the formation of hydrogen peroxide from superoxide (Fig. 4a and Figure S14a, lane 2). This was confirmed by the independent addition of hydrogen peroxide to the reaction of Fe(II)-**1** and DTT (Figure S15, lane 8), which showed a similar high actvity. Moreover, the addition of SOD in combination with catalase suppresses the reaction significantly (Figure S14a, lane 4), which proves that the hydrogen peroxide is formed by SOD. The presence of 'free' hydroxyl radicals was excluded; no inhibition was observed when DMSO was added to the reaction solution (Figure S15, lane 5). The presence of free hydrogen peroxide can be also excluded in the present system, since addition of catalyse does not give rise to a decrease in activity (Fig. 4a and Figure S14a, lane 3).

It is unlikely that superoxide radicals are the active species effecting hydrogen abstraction from the DNA, which starts the cascade of reactions resulting in DNA cleavage. While it is true that examples of direct hydrogen abstraction by superoxide radicals from substrates with readily transferable hydrogens, such as reduced flavins, hydrazines and hydroxyl amines, have been reported, these proceeded only in non-protic solvents, such as DMF.[43,44] Protonation of $O_2^{\bullet-}$ to give the conjugated acid HO_2, which is also capable of hydrogen abstraction, results in highly rapid decomposition.[45,46] Additionally, it has been demonstrated that DNA strand cleavage induced by KO_2 under physiological conditions is the result of the autocatalytic dismutation of superoxide into hydrogen peroxide, which can act as the terminal oxidant together with a metal ion.[47] Therefore, an interaction between Fe(II)–**1** and superoxide radicals to produce another active oxidant is more likely. It has been demonstrated that [Fe(EDTA)] can undergo a series of reactions with superoxide, in which superoxide acts both as a reductant and as an oxidant (Scheme S2†).[48,49] Importantly, this cascade of reactions results in the formation of free hydrogen peroxide, which has been identified as an important intermediate in the degradation of DNA by Fe(MPE).[50] Furthermore, it has been demonstrated that $[(N4Py)Fe^{III}(\eta^1\text{-}OOH)]^{2+}$ can undergo a reversible deprotonation with an appropriate base to give $[(N4Py)Fe^{III}(\eta^2\text{-}O_2)]^+$.[27] In principle, this latter species can also

be accessed *via* a direct reaction between superoxide and Fe(II)–**1**, and then gives rise to $[(N4Py)Fe^{III}(\eta^1\text{-}OOH)]^{2+}$ after protonation.

These observations combined give rise to the following mechanistic proposal. The first step is electron transfer (either inner- or outer-sphere electron transfer) of the iron(II) complex Fe–**1** to dioxygen, resulting in the formation of an iron(III) complex and a superoxide radical (Scheme 1a). Due to the high concentration of DTT (1.0 mM) in solution, the iron(III) complex is reduced back to an iron(II) complex (Scheme 1b). In principle, superoxide can be reduced under these conditions as well, since the formal reduction potentials for the iron complex and superoxide are comparable.[27,38,51] However, reduction of the iron(III) complex by DTT is essentially diffusion controlled, whereas the reduction of superoxide is proton coupled and, hence, is expected to show slower electron transfer kinetics. Hence, reduction of the iron(III) complex is most likely to be faster. This is supported by the observation that addition of catalase, which decomposes hydrogen peroxide, does not lead to reduced DNA cleavage (Fig. 4b). The reaction between the iron(II) complex and superoxide gives rise to the formation of an iron(III)-peroxo complex (Scheme 1c), which after protonation results in the formation of the low spin iron(III)–hydroperoxide complex. This species acts as either the terminal hydrogen abstracting species, by analogy to $[(BLM)Fe^{III}OOH]^{2+}$ ('activated bleomycin'),[40–42] or is the precursor for the active species by homolysis of the peroxide O–O bond as was demonstrated before in catalytic oxidation of organic substrates.[39]

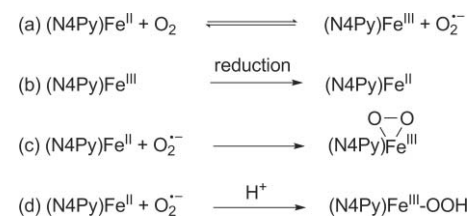

Scheme 1 Possible molecular oxygen activation route of Fe(II)–N4Py.

This proposal is supported by recent reports in which it was described that the $[(N4Py)Fe^{III}\text{-}OOH]^{2+}$ species can be generated by reaction of Fe(II)–**1** with O_2 in the presence of an NADH analogue and an acid as the source of electron and proton equivalents, respectively.[52] Moreover, through coupled electron and proton transfer, Fe(II)–N4Py complexes are able to activate and reduce O_2 in a completed catalytic cycle.[53]

The current hypothesis requires that both $[Fe^{II}(N4Py)]$ and superoxide radicals are present simultaneously. However, when no reductant is present, the reduction of Fe(III) to Fe(II) becomes rate limiting and, thus, the probability of such an encounter is low. This explains the lower reactivity and the different pattern of cleavage activity observed with the ROS scavengers in the absence of DTT. $[Fe^{II}(N4Py)]$ reacts with dioxygen to yield $[Fe^{III}(N4Py)]$ together with a superoxide radical. Since then there is very little Fe(II) present, most of the superoxide will decompose, which results in an overall lower activity. In the presence of SOD the superoxide formed is converted promptly into hydrogen peroxide. The remaining activity could be the result of interaction between $[Fe^{II}(N4Py)]$ or $[Fe^{III}(N4Py)]$ with H_2O_2.[38] A key observation to support this hypothesis is that a further drop in activity was observed upon addding SOD and catalase simultaneously (Fig. 4b and Figure S14b,† lane 4).

Conclusions

In this study it has been demonstrated that the DNA cleavage activity of N4Py iron complexes in the presence of a reductant can be modulated by varying the structure of the ligand. A series of new monotopic N4Py derived ligands have been designed and prepared. Their iron(II) complexes are capable of efficient oxidative DNA cleavage at low catalyst loading (150 bp/Fe(II)–N4Py). Structural modification of Fe(II)–N4Py complexes resulted in significantly different DNA cleavage behaviour in the presence of external reducing agent DTT. The nature and number of the DNA binding moieties and length of the linkers, all influenced the DNA cleavage activity of Fe(II)–N4Py. A small amount of direct double-strand DNA cleavage was obtained with Fe(II)–**3c** and Fe(II)–**4b**, which are the first examples of oxidatively achieving *dsc* with synthetic mononuclear iron complexes. In the absence of DTT, DNA cleavage with Fe(II)–N4Py complexes was much less efficient and the effect of structure on activity is less significant. It is proposed that this is caused by the fact that the rate limiting step in the absence of DTT is the reduction of Fe(III) back to Fe(II), instead of the DNA oxidation in the case when DTT is present. Inhibition experiments with different ROS scavengers and Fe(II)–**1** demonstrated that superoxide is being formed. A mechanistic proposal was put forward, in which the key point is the interaction of Fe(II)–N4Py with superoxide radicals to form Fe(III)–peroxo and (or) Fe(III)–hydroperoxide complexes, which are proposed to be the active species, or precursor. Considering the wealth of information about molecules capable of DNA binding and recognition,[54] this concept can be further extended to develop more active Fe(II)–N4Py complexes capable of direct double-strand DNA cleavage and sequence selective DNA cleavage for the synthetic mimics of Fe(II)–BLM.

Experimental section

General information

All reagents and solvents were used as purchased without further purification unless noted. Ligands **1**, **2** and **3a** were synthesized according to literature procedures and all data were in agreement with published ones.[25,26] NMR spectra were recorded on a Varian VXR-300 system. MS-ESI spectrometry was performed on a Triple Quadrupole LC/MS/MS spectrometer (API 3000, Perkin-Elmer Sciex Insruments). Melting temperatures were recorded on a Büchi B-545 melting point apparatus.

Bleomycin Sulfate ($A_2 + B_2$, 95%), from *Streptomyces verticillus*, was purchased from Calbiochem. Superoxide dismutase (SOD, from bovine erythrocytes) was purchased from Fluka, catalase (from bovine liver) was purchased from Sigma-Aldrich, and bovine serum albimum (BSA) was purchased from New England Biolabs (NEB). pUC18 plasmid DNA, isolated from E. coli XL1 Blue, was purified using QIAGEN maxi kits. Concentrations were determined by UV/Vis (A260) using a NanoDrop 1000 spectrophotometer (Thermo SCIENTIFIC). Restriction enzymes and restriction buffers were purchased from New England Biolabs (NEB). Agarose used for the gel electrophoreses was purchased from Invitrogen. Pictures of the gel slabs were taken with a Spot Insight CCD camera. The intensity of bands on the film were quantified using the software program Gel-Pro Analyzer

version 4.0.00.001. Statistic calculations were performed using Mathematica version 7.01.

DNA cleavage experiments

Iron(II) complexes of ligand **1** and **2** were dissolved in H_2O. 1 equiv. of $(NH_4)_2Fe^{II}(SO_4)_2{\cdot}6H_20$ was added to solutions of BLM, ligands **3a–c** and **4a–c** in H_2O to generate the corresponding iron(II) complexes *in situ*. 2% MeOH and DMF were used to help **3a–c** and **4a–c** dissolve in H_2O, respectively. The respective iron(II) complex solutions were added to a buffered solution (10 mM Tris·Cl, pH 8.0) of supercoiled pUC18 plasmid DNA with or without dithiolthreitol (DTT). The reaction solutions, with a final volume of 50 μL and a final concentration of 1.0 μM iron(II) complex, 0.1 μg μL^{-1} DNA (150 μM in base pairs) with or without 1.0 mM DTT, were incubated at 37 °C. Samples (2 μL) were taken from reaction solutions at the time points indicated, then quenched in 15 μL NaCN solution (1 mg mL^{-1}, containing 2040 equiv. NaCN with respect to Fe(II)–N4Py) with 3 μL loading buffer (consisting of 0.08% bromophenol blue and 40% sucrose, 6 × conc.) and immediately frozen in liquid nitrogen. The samples were run on 1.2% agarose gels in 1 × TAE buffer for at least 90 min at 70 V. Gels were stained in an ethidium bromide bath (1.0 μg mL^{-1}) for 45 min then washed with gel running buffer. Quantification was performed by fluorescence imaging and a correction factor of 1.31 is used to compensate for the reduced ethidium bromide uptake capacity of supercoiled plasmid pUC18 DNA.[28] All results were obtained from cleavage experiments that were performed at least in triplicate.

Calculation of amounts of *ssc* and *dsc*

The average number of single- (n) and double-strand cuts (m) in a DNA molecule were calculated using both Eqn (1) and Eqn (2),[55] in which f_{III} and f_I is the fraction of linear DNA and supercoiled DNA, respectively. Eqn (3) is the Freifelder–Trumbo relationship,[10a] in which h is the maximum distance in base pairs between nicks on opposite strands to generate a double strand cut (*i.e.* 16), and L is the total number of base pairs of the DNA used (2686 bp for pUC18 plasmid DNA). Uncertainties in the values of m and n were calculated by a Monte Carlo simulation as described previously.[28,29]

$$f_{III} = m \times e^{-m} \quad (1)$$

$$f_I = e^{-(m+n)} \quad (2)$$

$$m = \frac{n^2(2h+1)}{4L} \quad (3)$$

Calculation of cleavage rate

For single-strand DNA cleavage, the average numbers of single-strand cut per DNA molecule (n) can be calculated by using Equation (4) (when linear DNA is not present) or Equation (5) (when linear DNA is present). Uncertainty limits of the data are calculated based on a Monte Carlo simulation, taking into account a standard deviation of σ 0.03 for individual DNA fractions.¶ The calculated values of n can be plotted as a function of time, and the rate constant (k_{obs}) of single-strand DNA cleavage is determined from the linear fit of the graph. Values of k_{obs} are corrected into k^* by using Eqn (6) taking into account concentrations of DNA (0.1 μg μL^{-1}, 0.0564 μM) and iron complex (1.0 μM). (See ESI† for further details)

$$f_I = e^{-n} \quad (4)$$

$$f_I + f_{II} = [1 - n(2h+1)/2L]^{n/2} \quad (5)$$

$$k^* = k_{obs} \times \frac{[DNA]}{[complex]} \quad (6)$$

Synthesis of ligands

Ligands **1**, **2** and **3a** were prepared following published procedures.[25,26]

***N*-(6-Aminohexyl)-6-(((dipyridin-2-ylmethyl)(pyridin-2-ylmethyl)amino)methyl)nicotinamide (3b).** A solution of **5**[26] (620 mg, 1.45 mmol), 1,6-diaminohexane (2.03 g, 17.5 mmol) and NaCN (14 mg, 0.29 mmol) in MeOH (30 mL) was heated under reflux overnight under a N_2 atmosphere. After cooling to room temperature, the orange red reaction solution was poured into H_2O (250 mL) and the aqueous layer was washed with Et_2O (3 × 75 mL), extracted with CH_2Cl_2 (3 × 75 mL). The combined CH_2Cl_2 layer was washed with H_2O (50 mL), dried over Na_2SO_4 and evaporated to yield **3b** (592 mg, 80%) as a viscous yellow brown liquid. ^{1}H NMR (300 MHz, $CDCl_3$): δ = 8.79 (s, 1 H), 8.42 (d, J = 4.8 Hz, 2 H), 8.34 (d, J = 4.8 Hz, 1 H), 7.96 (dd, J = 7.8 Hz, 2.1 Hz, 7 H), 7.49 (m, 3 H), 7.01 (m, 3 H), 5.22 (s, 1 H), 3.89 (s, 2 H), 3.83 (s, 2 H), 3.26 (quart, J = 6.6 Hz, 2 H), 2.53 (t, J = 6.8 Hz, 2 H), 1.64 (br, N–H), 1.46 (m, 2 H), 1.23 ppm (m, 6 H); ^{13}C NMR (75 MHz, $CDCl_3$): δ = 165.5, 162.4, 159.4, 159.1, 148.9, 148.7, 147.3, 136.1, 136.0, 135.2, 128.5, 123.7, 122.7, 122.1, 121.9, 121.7, 71.6, 71.5, 57.0, 56.6, 41.7, 39.6, 33.2, 29.2, 26.4, 26.1 ppm; MS (ESI$^+$): m/z: 510.6, [M + H]$^+$, 532.5 [M + Na]$^+$.

6,6′-(Dipyridin-2-ylmethylazanediyl)bis(methylene)bis(*N*-(3-aminopropyl)nicotinamide) (3c). A solution of **8**[32] (330 mg, 0.69 mmol), 1, 3-diaminopropane (1.5 mL, 18 mmol) and NaCN (9 mg, 0.18 mmol) in MeOH (30 mL) was heated under reflux overnight under a N_2 atmosphere. After cooling to room temperature, the orange red reaction solution was concentrated by evaporation and the product was purified by size exclusion column chromatography (Sephadex LH 20/MeOH) to yield **3c** (243 mg, 62%) as a viscous red brown liquid. ^{1}H NMR (300 MHz, CD_3OD): δ = 8.75 (s, 2 H), 8.43 (d, J = 4.5 Hz, 2 H), 8.31 (dd, J = 8.1 Hz, 2.1 Hz, 2 H), 7.73–7.64 (m, 6 H), 7.23 (m, 2 H), 5.32 (s, 1 H), 3.98 (s, 4H), 3.40 (t, J = 6.6 Hz, 4 H), 2.66 (t, J = 6.8 Hz, 4 H), 1.72 ppm (m, 4 H); ^{13}C NMR (75 MHz, CD_3OD): δ = 167.9, 163.6, 160.8, 150.1, 148.6, 138.4, 136.9, 130.1, 125.7, 124.4, 124.1, 74.7, 74.6, 58.6, 39.8, 38.4, 33.2 ppm; MS (ESI$^+$): m/z: 284.7, [M + 2H]$^{2+}$; 568.3, [M + H]$^+$; 590.3 [M + Na]$^+$.

¶ The standard deviation was determined independently by 24 identical DNA oxidation experiments with Fe(II)–**1** and 0.03 is the largest value of standard deviation in experiments. See Ref. 28,29.

General procedure for the syntheses of ligands 4a, 4b and 4c. A mixture of 1,8-naphthalic anhydride and corresponding amine-substituted N4Py **3a**, **3b** and **3c** in MeOH (~10 mM) was heated under reflux overnight. After cooling down to r.t., the reaction mixture was filtered through cotton and the solvent was evaporated. The residue was purified by column filtration (Al_2O_3 neutral act. I, CH_2Cl_2–MeOH 1 : 1) to yield **4a**, **4b** and **4c**, respectively.

***N*-(3-(1,3-Dioxo-1*H*-benzo[*de*]isoquinolin-2(3*H*)-yl)propyl)-6-(((dipyridin-2-ylmethyl)(pyridin-2-ylmethyl)amino)methyl)nicotinamide (4a).** Starting from **3a** (200 mg, 0.43 mmol) and 1,8-naphthalic anhydride (93 mg, 0.47 mmol), **4a** (194 mg, 70%) was yielded as a light yellow brown solid. M.p.: 107 °C (decomp.); ^{1}H NMR (300 MHz, $CDCl_3$): $\delta = 9.08$ (d, $J = 2.1$ Hz, 1H), 8.63–8.50 (m, 5 H), 8.24 (d, $J = 8.1$ Hz, 2 H), 8.17 (dd, $J = 9.0$ Hz, 2.3 Hz, 1 H), 7.80–7.60 (m, 9 H), 7.18–7.11 (m, 3 H), 5.37 (s, 1 H), 4.33 (t, $J = 6.0$ Hz, 2 H), 4.06 (s, 2 H), 3.99 (s, 2 H), 3.45 (quart, $J = 5.8$ Hz, 2 H), 2.30 (s, N–H), 2.07 ppm (m, 2 H); ^{13}C NMR (75 MHz, $CDCl_3$): $\delta = 165.4, 164.8, 163.1, 159.8, 159.5, 149.3, 149.1, 147.6, 136.3, 135.3, 134.4, 131.7, 131.6, 128.3, 128.1, 127.0, 124.2, 123.1, 122.6, 122.2, 121.9, 72.3, 58.3, 57.5, 57.1, 37.4, 36.1, 27.7$ ppm (signals missing due to peak overlap); MS (ESI$^+$): m/z: 648.5, $[M + H]^+$.

***N*-(6-(1,3-Dioxo-1*H*-benzo[*de*]isoquinolin-2(3*H*)-yl)hexyl)-6-(((dipyridin-2-ylmethyl)(pyridin-2-ylmethyl)amino)methyl)nicotinamide (4b).** Starting from **3b** (280 mg, 0.55 mmol) and 1,8-naphthalic anhydride (123 mg, 0.62 mmol), **4b** (258 mg, 68%) was yielded as a light brown solid. M.p.: 131.0–132.8 °C; ^{1}H NMR (300 MHz, $CDCl_3$): $\delta = 8.91$ (s, 1 H), 8.58–8.55 (m, 4 H), 8.48 (d, $J = 4.8$ Hz, 1 H), 8.20 (d, $J = 8.1$ Hz, 2 H), 8.08 (dd, $J = 9.0$ Hz, 2.1 Hz, 1 H), 7.76–7.58 (m, 9 H), 7.16–7.07 (m, 3 H), 6.54 (br, N–H), 5.32 (s, 1 H), 4.18 (quart, $J = 6.8$ Hz, 2 H), 4.02 (s, 2 H), 3.95 (s, 2 H), 3.44 (quart, $J = 5.9$ Hz, 2 H), 1.77 (m, 2 H), 1.64 (m, 2 H), 1.48 (m, br, 4 H); ^{13}C NMR (75 MHz, $CDCl_3$): $\delta = 165.6, 164.1, 162.9, 159.7, 159.4, 149.1, 148.9, 147.3, 136.2, 136.1, 135.3, 133.8, 131.4, 131.0, 128.5, 127.9, 126.8, 123.8, 122.8, 122.4, 122.3, 122.1, 121.8, 71.9, 71.8, 57.3, 56.9, 39.8, 39.5, 29.1, 27.7, 26.1, 26.0$ ppm (signals missing due to peak overlap); MS (ESI$^+$): m/z: 690.5, $[M + H]^+$, 712.4 $[M + Na]^+$.

6,6′-(Dipyridin-2-ylmethylazanediyl)bis(methylene)bis(*N*-(3-(1,3-dioxo-1*H*-benzo[*de*]isoquinolin-2(3*H*)-yl)propyl)nicotinamide) (4c). Starting from **3c** (326 mg, 0.50 mmol) and 1,8-naphthalic anhydride (250 mg, 1.26 mmol), **4c** (292 mg, 63%) was yielded as a yellow solid. M.p.: 131.6–134.6 °C; ^{1}H NMR (300 MHz, $CDCl_3$): $\delta = 9.08$ (s, 2 H), 8.60–8.51 (m, 6 H), 8.21–8.16 (m, 6 H), 7.76–7.67 (m, 10 H), 7.19–7.14 (m, 2 H), 5.39 (s, 1 H), 4.30 (t, $J = 6.0$ Hz, 4H), 4.07 (s, 4 H), 3.44 (quart, $J = 5.6$ Hz, 4 H), 2.53 (s, N–H), 2.07 ppm (m, 4 H); ^{13}C NMR (75 MHz, $CDCl_3$): $\delta = 165.4, 164.7, 162.7, 159.7, 149.3, 147.7, 136.4, 135.3, 134.3, 131.6, 131.5, 128.5, 128.0, 127.0, 124.0, 122.7, 122.2, 122.1, 72.4, 57.3, 37.4, 36.2, 27.7$ ppm; MS (ESI$^+$): m/z: 928.5, $[M + H]^+$.

Acknowledgements

Financial support from the University of Groningen and the NRSC-Catalysis is gratefully acknowledged.

Notes and references

1 H. Umezawa, K. Maeda, T. Takeuchi and Y. Okami, *J. Antibiot.*, 1966, **19**, 200.
2 S. M. Hecht, Bleomycin: Chemical, *Biochemical and Biological Aspects*, Springer, New York, 1979.
3 W. K. Pogozelski and T. D. Tullius, *Chem. Rev.*, 1998, **98**, 1089.
4 R. M. Burger, *Chem. Rev.*, 1998, **98**, 1153.
5 S. M. Hecht, *J. Nat. Prod.*, 2000, **63**, 158.
6 H. Umezawa, *Biomedicine*, 1973, **18**, 459.
7 J. Stubbe, J. W. Kozarich, W. Wu and D. E. Vanderwall, *Acc. Chem. Res.*, 1996, **29**, 322.
8 J. Y. Chen and J. Stubbe, *Nat. Rev. Cancer*, 2005, **5**, 102.
9 L. Thompson, C. Limoli and C. Origin, *Recognition, Signaling and Repair of DNA Double Strand in Mammalian Cells*, Springer, New York, 2003.
10 (*a*) D. Freifelder and B. Trumbo, *Biopolymers*, 1969, **7**, 681; (*b*) R. Cowan, C. M. Collis and G. W. Grigg, *J. Theor. Biol.*, 1987, **127**, 229.
11 D. H. Petering, R. W. Byrnes and W. E. Antholine, *Chem.-Biol. Interact.*, 1990, **73**, 133.
12 R. P. Hertzberg and P. B. Dervan, *Biochemistry*, 1984, **23**, 3934.
13 D. S. Sigman, A. Mazumder and D. M. Perrin, *Chem. Rev.*, 1993, **93**, 2295.
14 R. J. Guajardo, S. E. Hudson, S. J. Brown and P. K. Mascharak, *J. Am. Chem. Soc.*, 1993, **115**, 7971.
15 R. J. Guajardo, F. Chavez, E. T. Farinas and P. K. Mascharak, *J. Am. Chem. Soc.*, 1995, **117**, 3883.
16 G. C. Silver and W. C. Trogler, *J. Am. Chem. Soc.*, 1995, **117**, 3983.
17 M. Pitié and G. Pratviel, *Chem. Rev.*, 2010, **110**, 1018.
18 P. Mialane, A. Nivorojkine, G. Pratviel, L. Azéma, M. Slany, F. Godde, A. Simaan, F. Banse, T. Kargar-Grisel, G. Bouchoux, J. Sainton, O. Horner, J. Guilhem, L. Tchertanova, B. Meunier and J. J. Girerd, *Inorg. Chem.*, 1999, **38**, 1085.
19 C. Marchand, C. H. Nguyen, B. Ward, J. S. Sun, E. Bisagni, T. Garestier and C. Hélène, *Chem.–Eur. J.*, 2000, **6**, 1559.
20 C. Hemmert, M. Pitié, M. Renz, H. Gornitzka, S. Soulet and B. Meunier, *JBIC, J. Biol. Inorg. Chem.*, 2001, **6**, 14.
21 E. L. M. Wong, G. S. Fang, C. M. Che and N. Y. Zhu, *Chem. Commun.*, 2005, 4578.
22 Q. Jiang, N. Xiao, P. F. Shi, Y. G. Zhu and Z. J. Guo, *Coord. Chem. Rev.*, 2007, **251**, 1951.
23 M. Roy, T. Bhowmick, S. Ramakumar, M. Nethaji and A. R. Chakravarty, *Dalton Trans.*, 2008, 3542.
24 Oxidative double-strand cleavage has been reported with Cu complexes, albeit with high copper/DNA base pair ratios: (*a*) F. V. Pamatong, C. A. Detmer, III and J. R. Bocarsly, *J. Am. Chem. Soc.*, 1996, **118**, 5339; (*b*) Y. Jin and J. A. Cowan, *J. Am. Chem. Soc.*, 2005, **127**, 8408; (*c*) J. He, P. Hu, Y. J. Wang, M. L. Tong, H. Z. Sun, Z. W. Mao and L. N. Ji, *Dalton Trans.*, 2008, 3207.
25 M. Lubben, A. Meetsma, E. C. Wilkinson, B. Feringa and L. Que, Jr., *Angew. Chem., Int. Ed. Engl.*, 1995, **34**, 1512.
26 G. Roelfes, M. E. Branum, L. Wang, L. Que, Jr. and B. L. Feringa, *J. Am. Chem. Soc.*, 2000, **122**, 11517.
27 G. Roelfes, V. Vrajmasu, K. Chen, R. Y. N. Ho, J. Rohde, C. Zondervan, R. M. la Crois, E. P. Schudde, M. Lutz, A. L. Spek, R. Hage, B. L. Feringa, E. Münck and L. Que, Jr., *Inorg. Chem.*, 2003, **42**, 2639.
28 T. A. van den Berg, B. L. Feringa and G. Roelfes, *Chem. Commun.*, 2007, 180.
29 R. P. Megens, T. A. van den Berg, A. D. de Bruijn, B. L. Feringa and G. Roelfes, *Chem.–Eur. J.*, 2009, **15**, 1723.
30 (*a*) Acridines are good intercalators into DNA , see: M. Wirth, O. Buchardt, T. Koch, P. E. Nielsen and B. Nordén, *J. Am. Chem. Soc.*, 1988, **110**, 932; (*b*) Ammonium ion has electrostatic interaction and hydrogen-bonding with the DNA phosphodiester backbone; (*c*) Naphthalimide unit is capable of both DNA groove binding and base pair intercalation, see: L. González-Bulnes and J. Gallego, *J. Am. Chem. Soc.*, 2009, **131**, 7781.
31 Previous reports have shown that the length of spacer has a strong influence on the activity of the complex to DNA cleavage. For examples, see: (*a*) S. Hashimoto and Y. Nakamura, *J. Chem. Soc., Perkin Trans. 1*, 1996, 2623; (*b*) E. Boseggia, M. Gatos, L. Lucatello, F. Mancin, S. Moro, M. Palumbo, C. Sissi, P. Tecilla, U. Tonellato and G. Zagotto, *J. Am. Chem. Soc.*, 2004, **126**, 4543.
32 See supporting information†.

33 K. D. Goodwin, M. A. Lewis, E. C. Long and M. M. Georgiadis, *Proc. Natl. Acad. Sci. U. S. A.*, 2008, **105**, 5052.
34 (*a*) J. M. McCord and I. Fridovic, *J. Biol. Chem.*, 1969, **244**, 6049; (*b*) M. S. Lah, M. M. Dixon, K. A. Pattridge, W. C. Stallings, J. A. Fee and M. L. Ludwig, *Biochemistry*, 1995, **34**, 1646; (*c*) G. C. Dismukes, *Chem. Rev.*, 1996, **96**, 2909; (*d*) C. K. Vance and A. F. Miller, *Biochemistry*, 2001, **40**, 13079.
35 A. J. Wu, J. E. Penner-Hahn and V. L. Pecoraro, *Chem. Rev.*, 2004, **104**, 903.
36 J. E. Repine, O. W. Pfenninger, D. W. Talmage, E. M. Berger and D. E. Pettijohn,, *Proc. Natl. Acad. Sci. U. S. A.*, 1981, **78**, 1001.
37 In the study of active Fe(II)–BLM intermediates, Rodriguez and Hecht observed inhibition effects in DNA cleavage activity and proposed the SOD may react directly with reactive Fe–BLM intermediates. L. O. Rodriguez and S. M. Hecht, *Biochem. Biophys. Res. Commun.*, 1982, **104**, 1470.
38 G. Roelfes, M. Lubben, K. Chen, R. Y. N. Ho, A. Meetsma, S. Genseberger, R. M. Hermant, R. Hage,S. K. Mandal, V. G. Young, Jr., Y. Zang, H. Kooijman, A. L. Spek, L. Que, Jr. and B. L. Feringa, *Inorg. Chem.*, 1999, **38**, 1929.
39 G. Roelfes, M. Lubben, R. Hage, L. Que, Jr. and B. L. Feringa, *Chem.–Eur. J.*, 2000, **6**, 2152.
40 R. M. Burger, J. Peisach and S. B. Horwitz, *J. Biol. Chem.*, 1981, **256**, 11636.
41 J. W. Sam, X. J. Tang and J. Peisach, *J. Am. Chem. Soc.*, 1994, **116**, 5250.
42 A. Decker and E. I. Solomon, *Curr. Opin. Chem. Biol.*, 2005, **9**, 152.
43 E. J. Nanni and D. T. Sawyer, *J. Am. Chem. Soc.*, 1980, **102**, 7591.
44 D. T. Sawyer and J. S. Valentine, *Acc. Chem. Res.*, 1981, **14**, 393.
45 B. H. J. Bielski, *Photochem. Photobiol.*, 1978, **28**, 645.
46 J. M. Gebicki and B. H. J. Bielski, *J. Am. Chem. Soc.*, 1981, **103**, 7020.
47 S. A. Lesko, R. J. Lorentzen and P. O. P. Ts'o, *Biochemistry*, 1980, **19**, 3023.
48 G. J. McClune, J. A. Fee, G. A. McCluskey and J. T. Groves, *J. Am. Chem. Soc.*, 1977, **99**, 5220.
49 C. Bull, G. J. McClune and J. A. Fee, *J. Am. Chem. Soc.*, 1983, **105**, 5290.
50 R. P. Hertzberg and P. B. Dervan, *J. Am. Chem. Soc.*, 1982, **104**, 313.
51 R. Y. N. Ho, J. F. Liebman and J. Selverstone Valentine, In *Active oxygen in biochemistry*, Ed. J. Selverstone Valentine, C. S. Foote, A. Greenberg, J. F. Liebman, Blackie A&P, Glasgow, 1995, pp. 2-4.
52 S. Hong, Y. M. Lee, W. Shin, S. Fukuzumi and W. Nam, *J. Am. Chem. Soc.*, 2009, **131**, 13910.
53 H. S. Soo, A. C. Komor, A. T. Iavarone and C. J. Chang, *Inorg. Chem.*, 2009, **48**, 10024.
54 For examples of DNA-binding units see: (*a*) E. R. Jamieson and S. J. Lippard, *Chem. Rev.*, 1999, **99**, 2467; (*b*) K. E. Erkkila, D. T. Odom and J. K. Barton, *Chem. Rev.*, 1999, **99**, 2777; (*c*) M. E. Vázquez, A. M. Caamaño and J. L. Mascareñas, *Chem. Soc. Rev.*, 2003, **32**, 338; (*d*) D. Jantz, B. T. Amann, G. J. Gatto, Jr. and J. M. Berg, *Chem. Rev.*, 2004, **104**, 789; (*e*) H. T. Chifotides and K. R. Dunbar, *Acc. Chem. Res.*, 2005, **38**, 146; (*f*) R. M. Doss, M. A. Marques, S. Foister, D. M. Chenoweth and P. B. Dervan, *J. Am. Chem. Soc.*, 2006, **128**, 9074; (*g*) M. J. Hannon, *Chem. Soc. Rev.*, 2007, **36**, 280; (*h*) A. D. Richards and A. Rodger, *Chem. Soc. Rev.*, 2007, **36**, 471; (*i*) D. R. Boer, A. Canals and M. Coll, *Dalton Trans.*, 2009, 399.
55 L. F. Povirk, W. Wübker, W. Köhnlein and F. Hutchinson, *Nucleic Acids Res.*, 1977, **4**, 3573.